iJRASET
International Journal For Research in
Applied Science and Engineering Technology

INTERNATIONAL JOURNAL FOR RESEARCH
IN APPLIED SCIENCE & ENGINEERING TECHNOLOGY

Volume: 11 Issue: XII Month of publication: December 2023

DOI: https://doi.org/10.22214/ijraset.2023.54439

International Journal for Research in Applied Science & Engineering Technology (IJRASET)
ISSN: 2321-9653; IC Value: 45.98; SJ Impact Factor: 7.538
Volume 11 Issue XII Dec 2023- Available at www.ijraset.com

A Study on Microstrip Array Antenna with FSS for Next Generation Cellular Communication

Palak Jain
Medicaps University Indore

Abstract: Fifth-generation wireless, often known as 5G, is the next version of cellular technology and is intended to provide major improvements to the speed and responsiveness of wireless networks. In addition, the increased bandwidth and improved antenna technologies that come with 5G make it possible for a significant increase in the quantity of data that can be transmitted via a wireless network. In order to build a successful next-generation cellular communication system in the terahertz (THz) regime, it is necessary to create high-directivity antennas, which will enable the signal to travel further than 0.1 km. This will allow the system to function effectively. Concurrently, large bandwidth antennas should be designed in order to facilitate the information's transmission.

Keywords: microstrip antenna, FSS, cellular communication

I. INTRODUCTION

In the field of communications, a microstrip antenna is often understood to refer to an antenna that was built on a printed circuit board using photolithographic processes. It may be thought of as an internal antenna. The microwave frequency range is where they are utilised the most. An individual microstrip antenna is made up of a patch of metal foil of varying shapes (also known as a patch antenna), which is adhered to the top surface of a printed circuit board (PCB), and a ground plane made of metal foil, which is adhered to the reverse side of the board. The vast majority of microstrip antennas are organised as arrays of numerous patches in two dimensions. Transmission lines made of foil microstrip are typically used to make the connection between the antenna and the transmitter or receiver. Between the antenna and the ground plane, either the radio frequency current is applied (or, in the case of receiving antennas, the received signal is created), or both.

Because of their thin planar profile, which allows them to be incorporated into the surfaces of consumer products, aircraft, and missiles; their ease of fabrication using printed circuit techniques; the ease of integrating the antenna on the same board with the rest of the circuit; and the possibility of adding active devices such as microwave integrated circuits to the antenna itself to make active antennas, microstrip antennas have become very popular in recent decades.

Microstrip antennas have a number of desirable characteristics, including a low profile, the ability to be flexible, a light weight, a tiny volume, and a low cost of manufacture. Integrating the RF feed network with the radiating components on the same substrate provides not only the benefit of a more compact and low-cost feed network, but also the ability to achieve this benefit. In the most recent decade, microstrip antennas have been the subject of several presentations in the form of books and articles. It is possible for communication networks, seekers, and biological systems to use microstrip antennas. In the next chapter, we will discuss numerous different uses for microstrip antennas. This chapter presents the design of high-efficiency mm-wave microstrip antenna arrays for use in this book's subsequent chapters. The gain restriction in microstrip antenna arrays that might occur as a result of feed network losses is presented by. This discussion, on the other hand, is restricted to a 12-gigahertz plane slot array, and neither radiation nor dielectric losses are taken into account. The term "patch antenna" refers to the type of microstrip antenna that is used the most frequently. There is also the possibility of constructing antennas that use patches as constituent elements in an array. A patch antenna is a narrowband, wide-beam antenna that is constructed by etching the antenna element pattern in a metal trace that is attached to an insulating dielectric substrate, such as a printed circuit board. A continuous metal layer that is glued to the opposite side of the substrate, which creates a ground plane, completes the construction of the patch antenna. Although square, rectangular, circular, and elliptical are the most common designs for microstrip antennas, any continuous shape is technically achievable. Some patch antennas do not make use of a dielectric substrate; rather, they are constructed of a metal patch that is placed above a ground plane using dielectric spacers; the structure that is produced by this method is less robust but has a broader bandwidth. Due to the fact that these antennas have a very low profile, are mechanically tough, and can be shaped to adapt to the curving skin of a vehicle, they are frequently installed on the outside of aeroplanes and spacecraft, in addition to being incorporated into mobile radio communications equipment. This is because of the fact that these antennas are able to conform to the curving skin of a vehicle.

II. LITERATURE REVIEW

Terahertz (THz) regime is a frequency band that runs generally between 0.1–10 THz and is placed between the millimeter-wave (mmWave) band and the infra-red (IR) band, as stated by [[1, [2], [3], [4], and [5]]. [[1], [2], [3], [4], and [5]]. To compensate for the path-loss of humid atmospheres, which can exceed over 100 dB/km, and to allow signal propagation for at least 100 m away, to maintain a short-range line-of-sight (LoS) communication system at this frequency regime, the establishment of cellular communications at THz is dependent on the development of high-power solid-state transmitter sources, low-losses connectors, and the most critical component in the evolution of high-directivity antennas. For instance, the impact of molecular absorption loss is significantly lower than 0.01 dB/m over frequency ranges ranging from 380 to 440 gigahertz. However, as a result of the spreading loss, the overall path-loss is extraordinarily large. As a consequence of this, high directivity antennas are required, in addition to the development of novel 3D massive multiple-input-multiple-output (MIMO) systems. Broadband antennas that are capable of transmitting information at a rate of at least 20 Gigabits per second need to be developed since the demand for high-speed data transfer is concurrently increasing by a factor of two every 18 months [6]. The International Telecommunication Union Radio (ITU-R) communication sector organisation did not standardise a frequency range over 275 GHz; yet, frequencies in this range can be utilised to transmit information at extremely high data speeds (tens of gigabits per second or even terabits per second).

According to [7], there are a few different technologies that offer high gain antennas. However, the microstrip antennas and horn antennas seem to be the most effective ones, since they permit efficiency exceeding 5 G in cellular communication. Horns feed are typically utilised as a source for lens and reflector antennas when operating at submillimeter wave frequencies (more than 0.3 THz) [8]. For the microstrip antennas, low-loss substrates, such as benzocyclobutene (BCB) polymer [9], are required to be used because of the frequency domain they operate in. The design and modelling of microstrip array antennas using substrate integrated waveguide (SIW) is the topic of this research article, which also discusses and studies these topics. These antennas need to have a maximum gain that is greater than 23 dB, while also having a radiating efficiency that is greater than 65% at resonance frequencies that fall between 108.3 and 114.7 GHz. The ANSYS HFSS solver should be utilised to perform software validation on this design. Consequently, the findings of the simulation will be accurate and near to the results that should be achieved at the experimental verification, which will help decrease the cost of the experimental validation. This will be accomplished by the manufacture of a prototype THz antenna.

V. Zhurbenko and colleagues modelled and simulated using the CST MWS solver a slow-wave structure antenna operating at a resonance frequency of 0.81 THz. This work was published in [10]. The greatest directivity and bandwidth that could be achieved were found to be 10.9 dBi and 220 GHz, respectively.

R. C. Diaz and colleagues modelled and simulated a scanning 8 1 waveguide apertures array antenna at a frequency of 0.275 THz using the ANSYS HFSS solver. This antenna was built for the purpose of experimental validation. The best BW that could be achieved was 110 GHz (40%).

Two distinct types of antennas were modelled and simulated using the ANSYS HFSS solver by E. Lacombe and colleagues in [12]. The frequency of the simulations was 0.23 THz. The first utilised a high density-interconnect (HDI) organic substrate at an antenna in package (Aip) structure, while the second utilised the same method with a lens. Both of these structures were referred to as antennas in packages. Fabrication of the first antenna was place for the purpose of experimental verification. The greatest directivity and bandwidth that could be attained were 5.5 dBi and 8.7% at 20 GHz for 17 dBi at 20 GHz respectively.

J. Xu and colleagues [13] modelled and simulated with the CST MWS solver a 140 GHz slot antenna array that featured a substrate integrated waveguide (SIW) with a resonance frequency of 140 GHz. Their work was published in the journal Communications of the IEEE. For the purpose of comparing the findings of the simulation with the experimental measurements, this antenna was manufactured from low temperature co-fired ceramic, abbreviated as LTCC. The largest boresight increases that could be attained were 15.6 dBi, and the bandwidth was increased to 25 GHz by 17.54 percent.

M. Alonso-delPino and colleagues modelled two micro-lens antennas operating at 1900 GHz in their paper [14]. These antennas consisted of a leaky-wave waveguide feeding and were constructed as a prototype using silicon micromachining and regular UV photolithography. The maximum directive, gain, bandwidth, and taper efficiency of the first and second models that were achieved were respectively, 33.5 dBi, 33.1 dB, 300 GHz (15.79%), 67.2%, and 41.2 dBi, 40.9 dB, 300 GHz (15.79%), 52.5%.

Modelling and simulation were performed on two end-fire on-chip antennas (OCA) at 0.14 THz and 0.32 THz by X. D. Deng and colleagues [15]. A prototype version of these antennas was created in the workshop. They utilised a silicon-germanium bipolar complementary metal-oxide-semiconductor (SiGe BiCMOS) technology with a standard thickness of 0.13 micrometres. For the first model, the maximum gain, bandwidth, and radiation efficiency were found to be 7 dBi, 70 GHz (48.2%), and 83%, whereas for the second model, they were 4 dBi, 40 GHz (12.5%), and 72%, respectively.

International Journal for Research in Applied Science & Engineering Technology (IJRASET)
ISSN: 2321-9653; IC Value: 45.98; SJ Impact Factor: 7.538
Volume 11 Issue XII Dec 2023- Available at www.ijraset.com

III. RADIATION OF A MICROSTRIP TRANSMISSION LINE

Figure 1 is an example of a microstrip transmission line, which consists of a flat conducting strip that is hung above a ground plane. Another example of this type of transmission line may be seen in Figure 2. The conducting strip is typically created by etching copper-clad material using photographic methods. This process requires that the conducting strip be supported by a dielectric substrate. Microstrip is a sort of gearbox line that offers an alternative to other types of gearbox lines that is both more affordable and more compact. It is utilised in the production of electronic components such as directional couplers, powers dividers and filters. These components are able to be simply combined with other circuit modules such as amplifiers, attenuators, and switches.

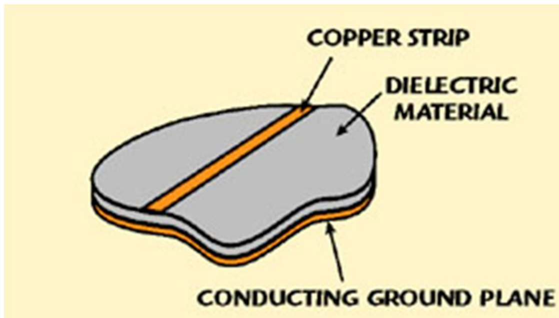

Fig 1: A microstrip transmission line

Because of the apparently uncontrollable radiation that occurred at microwave frequencies, microstrip circuits were initially only used for lower frequency applications (such as VHF or UHF). When ceramic substrates with tightly regulated high dielectric constants were available, this feature was able to be overcome, and the amount of radiation that was emitted was brought down to an acceptable level. For the most part, other types of transmission lines, such as waveguide and triplate, have been substantially phased out and replaced with microstrip in the production of microwave components and circuits. Applications that require a lot of electricity are an exception to this rule.

Radiation is something that happens naturally in microstrip circuits, and now that it is better understood, it is being used to our advantage in the construction of microstrip antennas. The realisation that radiating does not occur along straight stretches of microstrip line is essential to gaining a grasp of the mechanism of radiation. Even at microwave frequencies, it was determined through measurements that test pieces constructed with a low-dielectric substrate that had a thickness of several millimetres to have a low transmission loss. In most cases, the performance is restricted because of the contact with a coaxial line, which may permit radiation.

The utilisation of ultra-large, air-spaced microstrip lines to provide a controlled radio frequency environment for the testing of electrically tiny antennas is an excellent illustration of a scenario in which minimal radiation is an absolute must. Figure 2 depicts one embodiment, which is also a kind of TEM cell and may be found in some implementations. The gadget being evaluated is then positioned inside so that comparative measures of sensitivity may be obtained. As the operator moves about, radiation from the cell causes oscillations in the field within; however, this effect is eliminated at frequencies up to the limit where high order modes propagate.

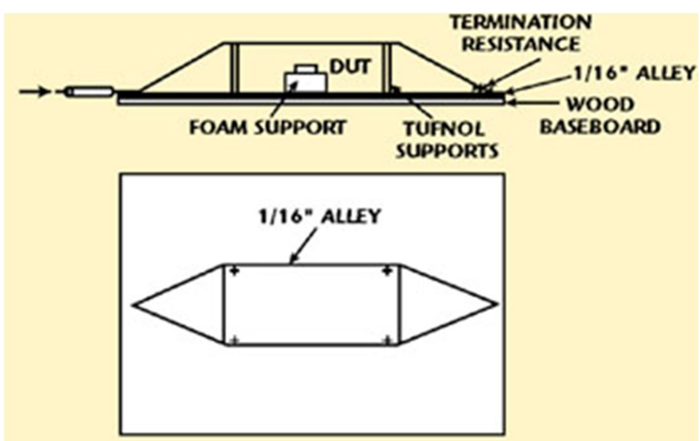

Fig 2: TEM cell configuaration

International Journal for Research in Applied Science & Engineering Technology (IJRASET)
ISSN: 2321-9653; IC Value: 45.98; SJ Impact Factor: 7.538
Volume 11 Issue XII Dec 2023- Available at www.ijraset.com

By examining the electric fields depicted in Figure 3, one may get a better understanding of why radiation is not allowed to occur in microstrip lines that are straight and why it does occur in microstrip discontinuities. The line's surrounding fields are balanced, which results in the cancellation of any radiated energy. The discontinuity emits a great deal of radiation near the terminal point of the line, where the electric fields are not in equilibrium. When wide transmission lines are utilised, the intensity of the radiation increases, and this effect is connected with thick substrates that have a low dielectric constant.

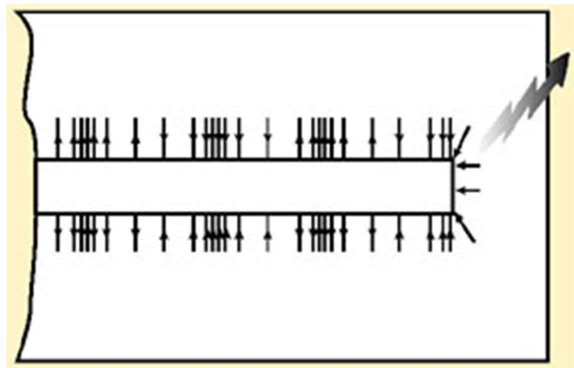

Fig 3: Microstrip fringing field

Figure 4 provides several examples of microstrip discontinuity for the reader to consider. Radiation is typically produced as a result of electric fields being out of equilibrium. Example d stands out as an exception since it features a connection that is properly balanced and does not emit radiation.

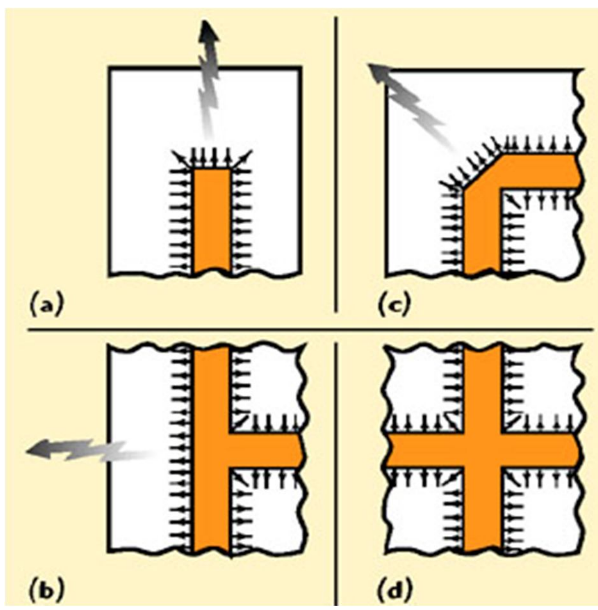

Fig 4: Microstrip discontinuities

Microstrip arrays may be created by "joining up" the admittances using straight microstrip lines, and the discontinuity can be represented by admittance where the radiation occurs. A significant portion of this course is dedicated to the characterization of discontinuities as well as the reciprocal coupling that exists between radiators.

IV. DESIGN METHODOLOGY

A. Microstrip Array Antenna with FSS

The structure of the antenna when modelled at a frequency of 114.7 GHz, where f0 stands for frequency zero, This antenna was constructed using the very same microstrip laminate as the planned 1st THz microstrip antenna, and it was built using the exact same parameters. This substrate was constructed using a SIW and the Wilkinson 1 x 32 power divider, as well as 20 x 32 circular radiations with inset-feds elements using the corporate-series fed approach.

The dimensions of the substrate were 72 millimetres by 60 millimetres by 0.127 millimetres, which equates to 27.53 by 22.94 by 0.048 at 114.7 gigahertz. At the microstrip antenna that was modelled and simulated, the frequency selective surfaces (FSSs) approach was employed to improve the directivity of the antenna. According to [16-17], FSSs are array structures that are made up of the vast majority of thin conducting components, and they are often supported by being placed on a dielectric substrate.

The array of dipoles and the array of slots, both of which are followed by a dielectric slab to produce FSSs, are the two fundamental varieties. These filters can either act as passive electromagnetic stop-band filters or pass-band filters. The performance of FSSs is primarily impacted by the surface roughness, dispersion, and ohmic losses while operating in the THz regimes. In addition, because of the resonant features of FSSs, they exhibit far more losses than a copper sheet does. Since of this, design considerations need to be taken into account since the transmission and reflection response of a periodic planar FSSs array is dependent on the geometry of the FSSs and the angle at which the waves are incident.

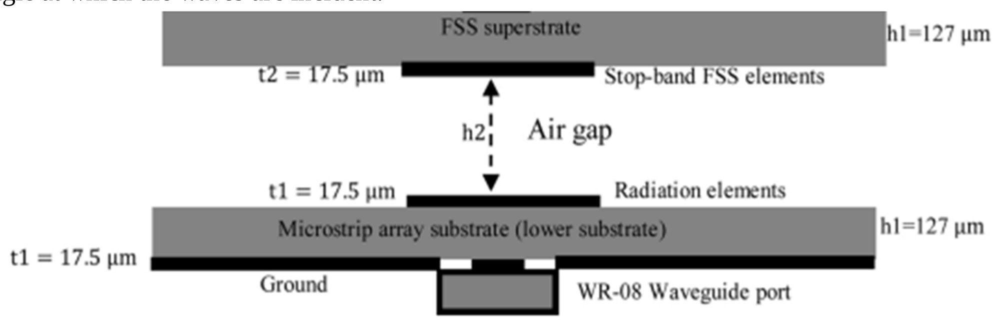

Fig 5: Formation of microstrip antenna with FSS.

The microstrip antenna with FSS has its fundamental construction illustrated here for your reference. The modelling and simulation of the third THz antenna took place at two PCBs. The first printed circuit board (PCB) had the radiation elements and the SIW, while the second printed circuit board contained the FSS superstrate with 26 stop-band FSS elements (double metallic rectangular ring with gaps) on Roger RO3003 dielectric microstrip substrate. There was a space filled with air in between the two substrates, and the distance between the FSS superstrate and the microstrip array substrate was denoted by the variable h2. Following optimisation performed with the CST MWS solver, the gap distance was adjusted to h2 = 0.95 mm = 0.347o@109.5 GHz. This was done in order to get the highest improvement in gain that could be achieved by including the FSS elements in the modelled antenna, each FSS element's size (a) need to be approximately smaller than the wavelength in the dielectric substrate.

B. Simulation Results

The results of the simulation of the modelled unit-cell stop-band in the FSS Figure 6 display the following set of findings from the simulation. These are the findings of the simulation for the reflection coefficient (S11) expressed in decibels for the modelled unit-cell stop-band FSS element.

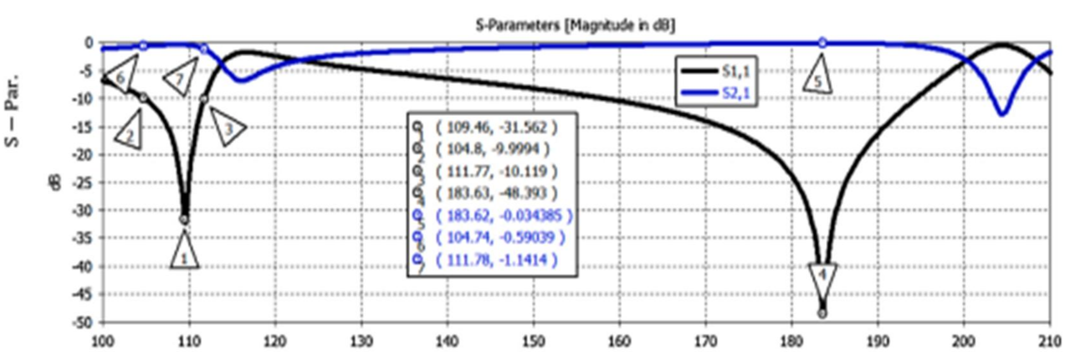

Fig 6: Simulation result for the reflection coefficient (S11) and the transmission.

For the frequency range of 104.8–111.76 GHz, it was demonstrated that the reflection coefficient was: S11 10 dB. Additionally, the simulation results of the transmission coefficient (S21) in (dB) of the modelled unit-cell stop-band FSS element are presented and described in the picture.

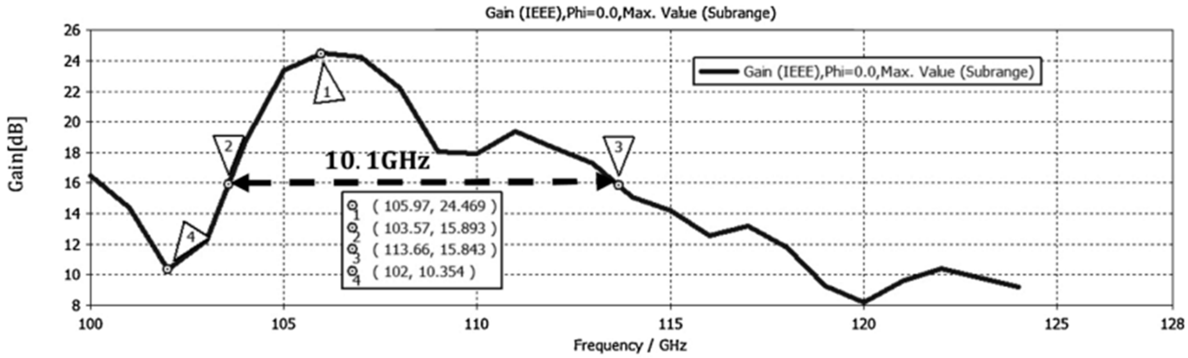

Fig 7: Simulation result of gain

The suggested THz antenna's frequency-dependent gain in (dB) is shown in Fig. 7 as a result of a 2D simulation. At frequencies between 102-116 GHz, it has been demonstrated that the gain ranged from 10.35 to 24.47 dB.

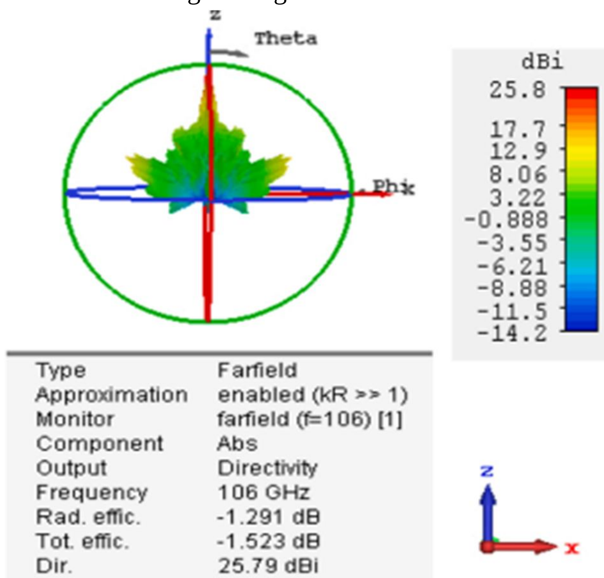

Fig 8: Simulation result of the directivity

The suggested THz antenna's 3D directivity simulation result at 106 GHz is shown in Fig. 8. It has been demonstrated that a directivity of 25.79 dBi was discovered.

V. CONCLUSION

Due to the straightforward 2-dimensional physical shape, microstrip antennas may be designed and produced at a reasonable cost. Due to the fact that the size of the antenna is directly related to the wavelength at the resonant frequency, they are often utilised at UHF frequencies and higher because of this relationship. A maximum directional gain of around 6–9 dBi may be achieved with a single patch antenna. Using lithographic methods, it is possible to print a number of patches on a single (big) substrate in a reasonably straightforward manner. Matching and phase correction may be achieved with printed microstrip feed structures, again in the same procedures that generate the radiating patches. Patch arrays can yield substantially larger gains than a single patch at very little additional expense. Patch arrays are utilised often in a variety of military applications, including aeroplanes, since they have the capacity to generate high-gain arrays despite their relatively modest profile.

REFERENCES

[1] K.R. Jha, G. Singh, Terahertz Planar Antennas for Next Generation Communication, Springer International Publishing Switzerland, 2014.
[2] K. Tekbiyik, A.R. Ekti, G.K. Kurt, A. Gorcin, Terahertz band communication systems: Challenges, novelties and standardization efforts, ELSEVIER Phys. Commun. 35 (2019) 1–18, 100700 May.
[3] I.F. Akyildiz, C. Han, S. Nie, Combating the distance problem in the millimeter-wave and terahertz frequency bands, IEEE Commun. Mag. 56 (June (6)) (2018) 102–108.

[4] I.F. Akyildiz, J.M. Jornet, C. Hana, Terahertz band: next frontier for wireless communications, ELSEVIER Phys. Commun. 12 (2014) 16–31.

[5] C. Han, Y. Chen, Propagation modeling for wireless communications in the terahertz band, IEEE Commun. Mag. 56 (June (6)) (2018) 96–101.

[6] S. Cherry, Edholm's law of bandwidth, IEEE Spectr. 41 (7) (2004) 58–60.

[7] B. Choudhury, A.R. Sonde, R.M. Jha, Terahertz Antenna Technology for Space Applications, Springer, New York, 2016.

[8] C. Wang, C. Lia, Q. Chen, B. Lu, X. Deng, J. Zhang, 10-Gbit/s wireless communication link using 16-QAM modulation in 140 GHz band, IEEE Microw. Wirel. Compon. Lett. 61 (7) (2013) 2327–2346.

[9] H. Vettikalladi, W.T. Sethi, A.F.B. Abas, Wonsuk Ko, M.A. Alkanhal, M. Himdi, Sub-THz Antenna for High-Speed Wireless Communication Systems, Hindawi Int. J. Antennas Propag. (2019) 1–9. March.

[10] V. Zhurbenko, V. Krozer, M. Kotiranta, T. Rubeek, Alain Durand, R. Marchesin, Submillimeter wave antenna with slow wave feed line, IEEE MTT-S International Microwave and Optoelectronics Conference (IMOC) (2009) 388–392.

[11] R.C. Diaz, S.V. Hoeye, C. Vazquez, G. Hotopan, M. Fernandez, F.L. Heras, Sub-millimeter wave frequency scanning 8×1 antenna array, Prog. Electromagn. Res. B Pier B 132 (2012) 215–232.

[12] E. Lacombe, F. Gianesello, C. Luxey, C. Durand, D. Titz, J.R. Costa, C. Fernandez, C. del Río Boccio, G. Ducournau, H. Gulan, T. Zwick, THz packaging solution for low cost Si-based 40 Gb/s wireless link system, 12th European Conference on Antennas and Propagation (2018) 1–3.

[13] J. Xu, Z.N. Chen, X. Qing, W. Hong, 140-GHz planar SIW slot antenna array with a large-via-fence dielectric loading in LTCC, in: IEEE 6th European Conference on Antennas and Propagation (EUCAP), March, 2012, pp. 3542–3545.

[14] M. Alonso-delPino, T. Reck, C. Jung-Kubiak, C. Lee, G. Chattopadhyay, Development of silicon micromachined microlens antennas at 1.9 THz, IEEE Trans. Terahertz Sci. Technol. 7 (March (2)) (2017) 191–198.

[15] X.D. Deng, Y. Li, H. Tang, W. Wu, Yong-Zhong Xiong, Dielectric loaded end-fire antennas using standard silicon technology, IEEE Trans. Antennas Propag. 65 (Febuary (6)) (2017) 2797–2807.

[16] F. Capolino, Theory and phenomena of metamaterials, Taylor & Francis Group (2009).

[17] B.A. Munk, Frequency Selective Surfaces - Theory and Design, John Wiley & Sons, New York, 2000.

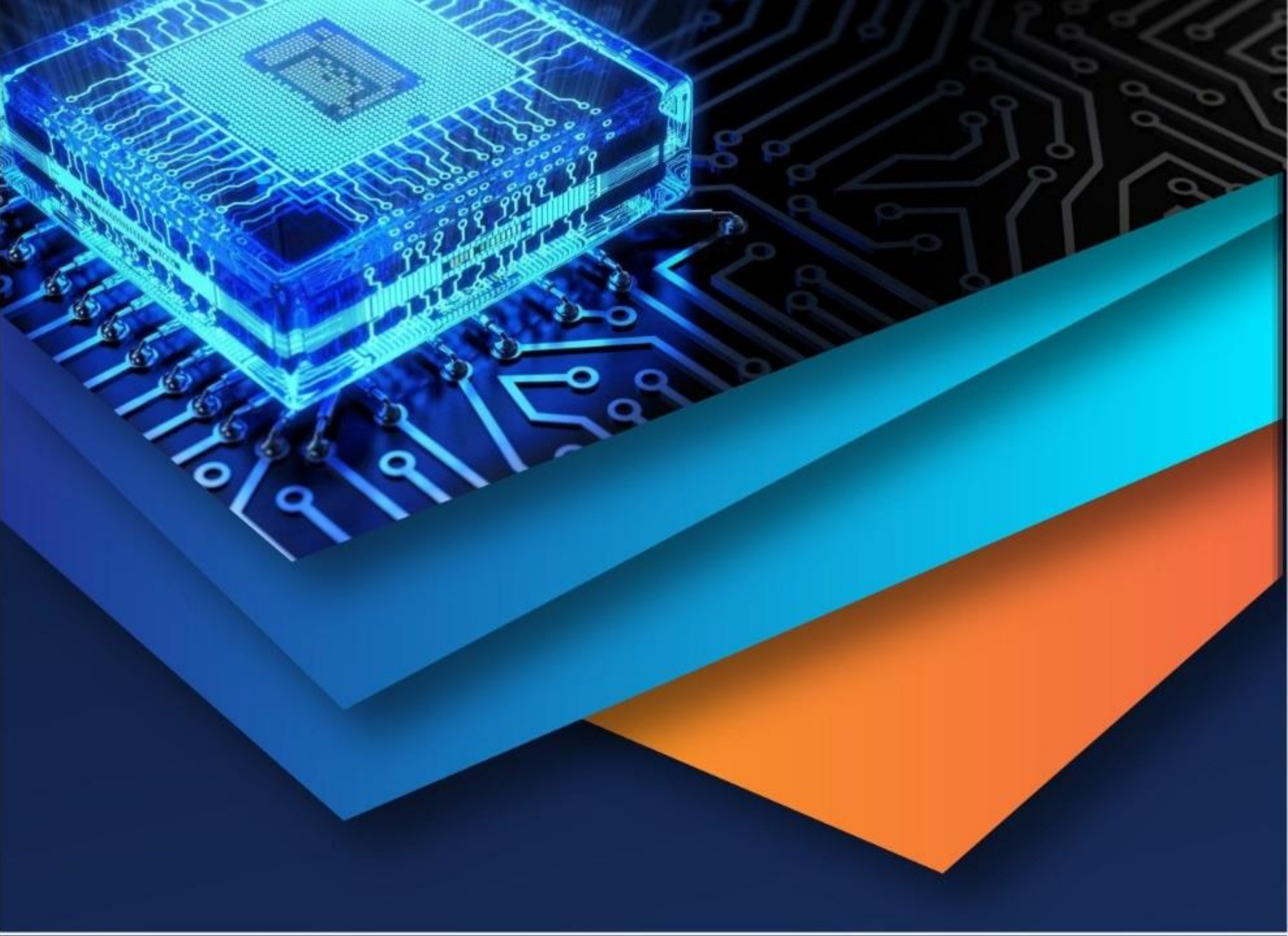

doi crossref

10.22214/IJRASET

INDEX COPERNICUS

45.98

ISRA JIF

IMPACT FACTOR: 7.129

TOGETHER WE REACH THE GOAL

IMPACT FACTOR: 7.429

ISI

INTERNATIONAL JOURNAL FOR RESEARCH

IN APPLIED SCIENCE & ENGINEERING TECHNOLOGY